CERN/TC/BEAM 66-2
14.3.1966

PRELIMINARY STUDY OF A RADIOFREQUENCY SEPARATED BEAM SU FOR THE SERPUKHOV ACCELERATOR

P. Bernard, P. Lazeyras, H. Lengeler and A.V. Samoilov

PS/5292/jc

INTRODUCTION

As a contribution to the Serpukhov - CERN collaboration, this report presents a preliminary study of a radiofrequency separated beam for bubble chamber experiments. It is the result of three months of common work, for which essential contributions of P.Bramham, B.Montague and D.Plane are gratefully acknowledged.

Although the technique of microwave particle separation is still relatively new, experience was gained at CERN during the design, tuning and operation of two beams, the O_2 and U_1. It was tried to apply this knowledge and experience to the quite different conditions of the Serpukhov accelerator.

The study was guided by some initial decisions inspired by the circumstances of the collaboration. It is assumed that an extracted proton beam will exist. The radiofrequency beam is designed specifically for bubble chamber experiments. The proposed techniques result from conservative extrapolations of present practice. The overall concept does not aim at reaching the highest possible energies, nor to provide maximum flexibility. The beam is intended as a first tool for bubble chamber experimentation with the Serpukhov accelerator, leaving ample room for future developments.

In many respects, the study has the character of an extrapolation, and suffers from the uncertainties always related to the exploration of a new domain. A number of reasonable assumptions were made, and safety factors were used correspondingly. Amongst these assumptions, there are

- the circulating proton intensity of the accelerator. As the beam is intended to work during the early stages of operation of the machine, the lower values of the existing estimates

were preferred;

- the cross sections for particle production. Some semi-empirical formulae, based on data from the accelerators now in operation, were extrapolated;
- the momentum resolution needed for high energy bubble chamber experiments. The experience available today is limited, especially in the large hydrogen bubble chambers operating at the highest energies reached up to now. The value adopted is possibly low, but a possible future relaxation of this requirement is doubtful and should be considered as a reserve.

It is hoped that the limitations of space and style that time imposes on the present report will not hamper its usefulness as a basis for future progress in the collaboration.

Yves Goldschmidt-Clermont

RADIOFREQUENCY PARTICLE SEPARATION

The separation of high energy particles is difficult: at present, the only possible and practical method is the radiofrequency separation, first proposed by Panofsky in 1959. This method, in the course of the following years, was developed theoretically and technically (e.g. 1 - 6), and was successfully performed experimentally at CERN (7, 8).

Shortly, the radiofrequency method is as follows:
A continuous beam of particles of momentum p passes successively through two regions of RF fields which exert a deflection force. The first field impresses onto the beam a high frequency structure which is analyzed in the second. The overall deflecting force on the particles is dependent on their time of flight between the two fields and thus on their rest mass, thereby enabling the separation of different kinds of particles.

The deflection is produced by a linearly polarized travelling wave ($\lambda \sim 10.0$ cm) supported by waveguides similar to those used in linear electron accelerators. The RF power needed to deflect high energy particles ($p > 10$ GeV/c) by an angle of about 1 mrad lies in the region of 10-20 MW. With current RF generators, such high powers can only be achieved for pulse durations of some µsec. As the beam pulse passing through the separator must obviously be shorter than the RF pulse duration, only fast ejected beams of the accelerator (having a pulse duration of 10 nsec to 2 µsec) can be used in conjunction with RF separators.

These beam bursts are still long compared to the period of the RF fields whose frequency lies around 3000 MHz.

Figure 1 illustrates the principle of operation of an RF separator with two deflecting structures. A momentum analysed beam passes successively through two deflecting waveguides. The distance between the waveguides is large compared to their length. For simplicity we assume that the beam has negligible angular divergence. The relative phase of the RF fields in the waveguides RF 1, RF 2 is kept constant and can be adjusted to any value. Midway between the two waveguides, is a beam optical system which images the centre of RF 1 with unity magnification into the centre of RF 2.

Imagine a beam of kaons and pions of same momentum p passing RF 1 along the axis. The particles receive a deflection $\varphi \sin \omega t$ depending on the field amplitude and on the entry phase ωt (φ : maximum deflection in one cavity, ω : angular frequency of RF fields).

Behind RF 1 the beam has a fan-shaped form with half opening angle φ and is modulated in angle as $\sin \omega t$ (cf., Fig. 1a where the trajectories of particles with different ωt are represented). If the cavities are short enough, the transit time difference of the two kinds of particles is very small and the deflection is practically independent of the particle rest mass. (This is in contrast to the electrostatic separator where spatial separation is achieved by the difference in transit time of two kinds of particles in a "long" electrostatic field).

The beam optical system transforms the deflections to $-\varphi \sin \omega t$. We adjust the relative phasing of RF 2 with respect to RF 1 in such a way that tne entry phase of a pion (unwanted particle) is the same in RF 2 as in RF 1. Then its second deflection will cancel the first one, provided the field amplitudes in RF 1 and RF 2 are equal. All pions will then be brought back to the axis, independently of their entry phase ωt. Fig. 1b represents the case $\omega t = 90^{\circ}$.

A kaon, passing RF 1 at the same moment as a pion will arrive at RF 2 with a time delay corresponding to a phase difference because of its greater rest mass. Its final deflection will be

$$\begin{aligned} \varphi_W(t) &= -\varphi \sin \omega t + \varphi \sin (\omega t + \tau) \\ &= 2\varphi \sin \frac{\tau}{2} \cos \left(\omega t + \frac{\tau}{2}\right) \end{aligned} \qquad [1]$$

The deflection of the kaon beam is thus modulated as $\sin \omega t$, the maximum value being $\varphi_W = 2 \varphi \sin (\tau/2)$, and the kaons emerge from RF 2 again in a fan-shaped distribution. At some distance behind RF 2 there is a centrally placed beam stopper whose thickness is chosen to intercept all pions (unwanted particles). It also intercepts some of the kaons (wanted particles) which are swept across it. However, if the peak deflection φ_W is big enough, most of them will pass the beam stopper and thereby spatial separation is achieved. The most favourable case is obtained for $\tau = 180^{\circ}$, then the deflection φ is just doubled in RF 2.(Cf., Fig.1b).

The accuracy of this time of flight method is given essentially by the frequency of the RF fields, half a period corresponding to about 0.15 nsec.

If the beam opening $\pm \delta$ at the entry of RF 1 is not negligible, the maximum deflection of the wanted particles behind RF 2 is $\delta + 2\varphi$ whereas the divergence of the unwanted-particle-beam is again $\pm \delta$. The thickness of the beam stopper has to be made corresponding at least to $\pm \delta$ in order to stop all unwanted particles.

A beam designed for microwave separation needs, in addition, the optical elements required to collect the particles emerging from the target, to perform the momentum analysis by magnetic deflections, and to improve as much as possible the separation of the desired particles from the unwanted ones.

If the RF cavities use linearly polarized waves, the momentum analysis can be done in the horizontal plane and mass analysis in the vertical plane; this eases considerably the tolerances on lens aberrations and on isochronism in the plane of momentum analysis.

INTENSITY CALCULATIONS

1) Cross sections

To obtain production cross-sections for primary proton energies of the order of 70 GeV/c we use an extrapolation formula for pions given by Trilling (9).

$$\frac{d^2N}{dpd\Omega} = A_1 p^2 \exp\{ -A_2\frac{p}{\sqrt{p_o}} - A_3 p\sqrt{p_o}\,\theta^2 \} \quad [1]$$

$$B_1\frac{p^2}{p_o}\exp\{ -B_2\left(\frac{p}{p_o}\right)^2 - B_3 p\theta \}$$

N : number of pions per interacting proton

p : secondary momentum in GeV/c

p_o : primary proton momentum in GeV/c

θ : production angle.

In this formula the hypothesis of constant transverse momentum and the decay of isobars are included.

Ranft (10) has fitted by a least-square method the coefficients A and B to the experimental cross-sections of Dekkers et al (11) at p_o = 23,1 GeV/c and for Be as target material. The values are given in Table 1.

TABLE 1

	A_1	A_2	A_3	B_1	B_2	B_3
π^+	1,67	3,76	4,23	1,76	10,21	4,28
π^-	1,50	3,76	4,23	0,604	10,21	4,28

The cross-sections obtained from formula [1] are given in Fig. 2. They are somewhat higher than values obtained by the v.Dardel extrapolation formula (12).

For the cross-sections of other particles we use the following ratios obtained also from extrapolations at lower energies

$$\frac{K^-}{\pi^-} = 0,05 \qquad \frac{K^+}{\pi^+} = 0,1 \qquad \frac{\bar{p}}{\pi^-} = 0,01 \quad [2]$$

It does not seem worthwhile to look for more detailed expressions when these ratios are used in connection with formula [1].

2) Particle intensities of the beam

In calculating particle intensities we keep in mind the results obtained in the CERN U_1-Beam which is very similar to the SU-beam. We also assume the same kind of two-deflector-separator as the one used in the O_2 and U_1 beams (5-6).

The estimates of the number of circulating protons in the Serpukhov accelerator range from 10^{11} to 10^{12} protons per burst. As the present study is intended for a beam working during the initial operation of the accelerator, we base our calculations on 10^{11} protons/burst, although this number could become substantially higher later on.

We assume a fast ejection system enabling zero angle production. As for bubble chamber experiments in the foreseen energy range of 10-40 GeV/c (see below) a momentum bite smaller than 1 o/o would be desirable, we assume a target size of only 2 x 2 mm^2 cross-section and about one interaction length. Comparing this with the emittance of the primary proton beam, it seems reasonable to assume that only about 10 o/o of the protons will hit the target. Furthermore 70 o/o of the secondaries produced in the right momentum and angle interval will be lost by reabsorption and Coulomb scattering.

The acceptance of the beam (including losses on collimators) is fixed to be 10^{-4} sterad, the momentum bite to be $\pm$ 0,25 o/o. Losses on the beam-stopper are assumed to be 85 o/o for $\bar{p}$ and 70 o/o for all other particles. Finally the distance between target and bubble chamber is fixed at 500 m (see below).

Under these assumptions the values of Fig. 3 and Fig. 4 are obtained.

3) Separation Energies

As is well known a two-deflector-separator can separate two kinds of particles from a third one only for some well defined energies, the only exception being separation of anti-protons at "high" energies (2, 13). In fixing the energies of separation we have to take into account the intensities of wanted particles, the distance between the two deflectors and their length.

a) if we accept the particle intensities given in Fig. 3 and Fig. 4 and if we assume that at least 10 wanted particles should reach the bubble chamber, it is obviously interesting to separate K^- and $\bar{p}$ up to 55 GeV/c and K^+, π^+ even above 60 GeV/c.

b) The phase difference between two particles of rest energy W_{o1}, W_{o2} over a distance L is given by (5)

$$\tau_{12} = \frac{\pi L}{\lambda} \quad \frac{(W_{o1}^2 - W_{o2}^2)}{(p\,c)^2} \qquad [3]$$

λ : wavelength of deflecting fields

p : momentum

We call design momentum p_o that momentum where the phase difference between a kaon and a pion is exactly π. From formula [3] one can calculate L for a given design momentum.

$$L = \frac{\lambda\,(p\,c)^2}{W_{o1}^2 - W_{o2}^2} \qquad [4]$$

In the CERN-separator λ = 10,5 cm, from [4] one gets L = 50 m for a design momentum of 10 GeV/c.

In Table 2 we note the values of L for various design momenta and for λ = 10,5 cm. One realises that the distances involved become rapidly prohibitive. One could consider reducing these distances by choosing a smaller value of λ e.g. λ = 3 cm. Unfortunately this is not advisable from the point of view of acceptance and also because there seem to be no microwave tubes available giving high energy.

TABLE 2

Distance L between deflectors, m

p_o, GeV/c	10	20	23	25	30	40
L, m	50	200	265	310	450	800

TABLE 3

Maximum separation energies, GeV/c

p_o, GeV/c		10	20	23	25	30	40
K^+_-	a.	14,3	28,6	33	35,8	42,9	57,2
$\bar{p}$	a.	7,3	14,6	16,8	18,2	21,9	29,2
	b.	> 20	>40	> 46	>50	> 60	(>80)
π^+	a.	8,7	17,4	20	21,7	26,1	34,8
	a.	~ 12	~24	~27,6	~30	~ 36	~48
	b.	~ 20	~40	~46	~50	~ 60	(~80)

a. Double particle rejection b. Single particle rejection

As for various reasons the beam-length should not exceed very much 500 m and there should be enough space for two momentum analyses, we are limited to about 300 m in the distance L.

c) The maximum deflection angle in one cavity should be of the order of 1 mrad to ensure good purity of the separated beam.

$$\varphi_{max} = \frac{c\bar{E}l}{pc} \qquad [5]$$

where $\bar{E}$: mean deflecting field

l : length of deflector.

Extrapolation of the experimental results from the CERN RF-separator (whose deflector length is 3m) shows that with a deflector of 6 m length fed by two r.f. power sources of 18 MW peak each, one can achieve about 32 MeV/c transverse momentum. This gives a deflection angle of 0.8 mrad at 40 GeV/c. The deflecting cavity can be divided into two 3m. lengths each fed by one r.f. source, so that no part of the waveguide system carries more than 18 MW. Higher deflection angles could be achieved by using higher field strengths $\bar{E}$. Unfortunately the peak value of $\bar{E}$ cannot be made substantially larger than the ones corresponding to 18 MW. Therefore the only way to increase φmax is to increase the deflector length.

In Table 3 we have noted the maximum separation energies for various design momenta and various kinds of particles. One can always make these energies smaller by decreasing L. From Table 3 and the previous arguments, we conclude that a design momentum of about 23 GeV/c seems to be a good compromise. We then lose the possibility of separating $K^{\pm}$ above 33 GeV/c and π^{+} above 46 GeV/c. Separation of $K^{\pm}$ up to ~60 GeV/c would not only involve too high an inter-cavity distance but also longer deflection, e.g.

Separation of K^{+} at 57 GeV/c gives L = 800 m

and a deflector length of about 10 m. Such a deflector not only needs three 20 MW-klystrons but also quite tight tolerances in the value of phase velocity in the structures.

4) Separator tolerances

The finite momentum bite of the beam introduces a phase spread in the particles between the cavities. It is given by

$$\Delta\tau = 2\pi \frac{L}{\lambda} \quad \frac{\Delta p}{p} \quad \frac{1}{\gamma^2} \qquad [6]$$

$\gamma^2 = \frac{1}{1-\beta^2}$ and introduces a broadening of the unwanted particle image on the beam-stopper. It is greatest in the case of 20 GeV π^+ separation: the maximum phase error of the protons is $\Delta\tau = 12^\circ$. The corresponding broadening of the beam-stopper is about 21 o/o giving 10 o/o additional losses of wanted particles.

In a 6m-structure the phase slip between wave and particles must be considered. It reduces the deflection of particles. This of course is undesirable for the wanted particles. For $\bar{p}$ at 17 GeV the phase slip is 18° giving a reduction in deflection angle of 3 o/o. But if one used the same separator at 10 GeV $\bar{p}$ the reduction in amplitude would be 15 o/o. It can however be avoided by reducing the phase velocity: anyway enough deflection angle is available at lower energies.

In the separator a phase constancy between the two structures of better than $\pm$ 2 o/o should be achieved (14). Bramham (15) shows that the system at present used in the CERN-Separator could cope with an inter cavity distance up to 500 m.

BEAM DESIGN

As can be seen from the above, to obtain a well separated beam we need a certain beam configuration. The necessary characteristics of the beam can be provided with the help of the following elements:

a) collimators

b) quadrupole lenses

c) bending magnets.

As with the Serpukhov accelerator, we enter a new energy range, it appears necessary to re-examine the determination of the parameters for each of these elements:

a) Collimators : they play the role of diaphragms bordering the beam in those places where it is necessary. As diaphragms, they must prevent unwanted particles to enter the bubble chamber, i.e., particles with wrong momenta, with divergences different from those required etc.

In this sense, the energy lost by traversing the walls of the collimators must be related to the expected momentum resolution. Of course, one must take into account a safety factor as it is impossible to foresee all the cases to be encountered in practice. However, if one assumes this reserve of safety not to exceed $\Delta p/p \sim 2$ o/o, then it appears that a reasonable choice for the collimator length is approximately 1 m of Cu. Incidentally, the ratio of this collimators length to the length of the CERN standard collimators is approximately equal to the ratio of energies of the Serpukhov and the CERN accelerators.

b)-c) Quadrupole lenses and bending magnets : These elements are more or less similar in characteristics to the corresponding CERN standard elements. Of course, the details of the technical execution of these elements will present some differences in characteristics, but one can hardly expect that these differences will be very significant. Therefore, for simplicity, we have considered that the effective length of each element (lenses and magnets) is equal to the iron length plus the aperture width. Such an approximation will need in the future certain corrections, but differences of 5-10 o/o from the precise characteristics cannot, essentially, change the overall picture. Preliminary characteristics of the quadrupole lenses and bending magnets which have been used for the computations are given in Table 4.

As an example of a possible solution, one can consider a magnetic channel whose optical scheme and lay-out are given in Fig. 5, and whose final characteristics are shown in Table 5.

TABLE 4

A) Quadrupoles

Q	Type	d mm	Z mm	L mm	X x Y mm²	G gauss/cm	P KW
1	7 K 135	70	1350	1430	355 x 290	3000	190
2	10 K 100	100	1000	1300	566 x 850	2000	60
3	10 K 200	100	2000	2230	566 x 850	2000	100
4	20 K 100	200	1000	1310	920 x 1225	1300	260
5	20 K 200	200	2000	2350	920 x 1225	1300	450

d diameter of quadrupole aperture — X outside width
Z length of pole piece — Y outside height

B) Bending magnets

M	Type	h x s mm²	Z mm	L mm	X x Y mm²	B gauss	P KW
1	SP - 129	100 x 240	4000	4750	1360 x 926	18,000	240
2	SP - 12A1	200 x 500	3000	4400	2200 x 1152	18,000	350
3	SP - 7A1	200 x 500	6000	7500	2600 x 1480	18,000	500

h magnet gap — Z length of pole piece — X outside width
s width of pole piece — L outside length — Y outside height

TABLE 5

FH - Horizontal focusing
DH - Vertical focusing
DL - Drift length between the centers of the elements
Q - Quadrupole lens
M - Bending magnet
A - Aperture (cm)
S - Effective length (cm)
FP - Focal point
- Bending angle (degrees)

Designed momentum p_o = 23 GeV/c.

No.	Element	Gradient(gs/cm) Field (Kgauss) Length (m)	Function	Other characteristics	Remarks
1	2	3	4	5	6
1	T	-	Target	-	2 x 2 x 150 mm^3
2	L	10	DL	-	-
3	Q1	760.3	FH	A = 20, S = 210	-
4	L	2.5	DL	-	-
5	Q2	648.8	DH	A = 20, S = 210	-
6	L	2.5	DL	-	-
7	Q3	648.8	DH	A = 20, S = 210	-
8	L	2.5	DL	-	-
9	Q4	760.3	FH	A = 20, S = 210	-
10	L	5.25	DL	-	-
1	M1	5.831	BM	A=20x50, S= 620	φ = 2.7
2	L	8	DL	-	-
3	M2	5.831	BM	A=20x50, S = 620	φ = 2.7
4	L	11	DL	-	Horizontal FP
5	L	2	DL	-	-
6	Q5	839.5	FH	A = 10, S = 110	Field lens
7	L	13	DL	-	-
8	M3	5.831	BM	A=20x50, S = 620	φ = 2.7
9	L	8	DL	-	-
20	M4	5.831	BM	A=20x50, S = 620	φ = 2.7

/contd.

TABLE 5 (contd.)

1	2	3	4	5	6
21	L	5.25	DL	-	
2	Q7	749.1	FH	A = 20, S = 210	-
3	L	2.5	DL	-	-
4	Q8	725.4	DH	A = 20, S = 210	-
5	L	23	DL	-	Horizontal and vertical FP's
6	L	23	DL	-	-
7	Q9	409.6	FH	A = 20, S = 210	-
8	L	5	DL	-	-
9	Q10	335.6	DH	A = 20, S = 210	-
30	L	209	DL	-	-
1	Q11	335.6	DH	A = 20, S = 210	-
2	L	5	DL	-	-
3	Q12	409.6	FH	A = 20, S = 210	-
4	L	23	DL	-	Horizontal and vertical FP's
5	L	12	DL	-	-
6	Q13	620.4	DH	A = 20, S = 210	-
7	L	2	DL	-	-
8	Q14	620.4	DH	A = 20, S = 110	-
9	L	2	DL	-	-
40	Q15	565.3	FH	A = 20, S = 210	-
1	L	2	DL	-	-
2	Q16	565.3	FH	A = 20, S = 110	-
3	L	16	DL	-	Vertical FP
4	L	2	DL	-	Horizontal FP
5	L	8	DL	-	-
6	Q17	657.4	DH	A = 20, S = 210	-
7	L	2	DL	-	-
8	Q18	657.4	DH	A = 20, S = 110	-
9	L	2	DL	-	-
50	Q19	566.2	FH	A = 20, S = 210	-
1	L	2	DL	-	-
2	Q20	566.2	FH	A = 20, S = 110	-
3	L	4.75	DL	-	-
4	M5	5.831	BM	A=20x50, S = 620	φ = 2.7

/contd.

TABLE 5 (contd.)

1	2	3	4	5	6
55	L	8	DL	-	-
6	M6	5.831	BM	A=20x50, S = 620	φ = 2.7
7	L	9	DL	-	Horizontal FP
8	L	2	DL	-	Vertical FP
9	L	20	DL	-	-
60	Q21	756.8	FH	A = 20, S = 210	-
1	L	2.5	DL	-	-
2	Q22	629.9	FH	A = 20, S = 210	-
3	L	20	DL	-	Horizontal FP
4	BC	-	-	-	Bubble chamber

The starting point for obtaining these results was as follows:

1) The optical scheme of the channel must be as simple as possible, i.e., consist of the least possible number of elements. This gives us a certain hope that the channel can be tuned rather easily and quickly.

2) To a certain extent one has used optical configurations which were already considered and experimented at CERN. One cannot say, of course, that the CERN channels are absolutely perfect, but they proved to be tunable, and well adapted to physics experiments.

The magnetic optical equipment of the channel consists of the following elements :

6	magnets with a 6 m path length and with a 20 x 50 cm^2 aperture:
16	2 m quadrupole lenses with a 20 cm aperture and maximal gradient of 1300 gs/cm:
4	1 m quadrupole lenses with a 20 cm aperture and maximal gradient of 1300 gs/cm:
1	1 m quadrupole lens with a 10 cm aperture and gradient of 2000 gs/cm:
9	1 m collimators:
1	beam stopper.

Quadrupole lenses with such gradients provide focusing of particles with a momentum of up to 40 GeV/c, the magnets give the possibility to transport along the channel particles with a momentum of up to 70 GeV/c. This last figure is important to permit the transport to the same bubble chamber, of particles with momentum approaching the maximum of the accelerator, without lenghty and costly modifications connected with the construction and tuning of a new beam, by requiring only the simpler task of a change in the lay-out and gradients of lenses. On the other hand, such a solution gives us the possibility to obtain particles with other energies, produced by protons at other places, and leading to the same bubble chamber or acting on other apparatus placed in the vicinity, but in the same direction.

The calculation of the beam characteristics, whose optical scheme is shown in Fig. 5, has been worked out with the help of the standard TRAMP programme (16). Experience gained at CERN shows that the experimental characteristics of the channels, which have been calculated with the TRAMP programme, differ from the calculated ones by no more than 1 o/o.

OPTICAL LAYOUT

Let us consider in more detail the above optical scheme. It consists of the following parts :

a) the target;

b) the first objective, which provides acceptance of particles coming from the target at a solid angle as large as possible;

c) the first momentum analyzer, providing a momentum resolution which is necessary for bubble chamber physics;

d) the second objective, which focuses the beam in the centre of the first RF cavity, thus providing a necessary linear magnification in the vertical plane;

e) the optics between RF1 and RF2, which must be described by a matrix in the vertical plane, equal to

$$M_V = \begin{bmatrix} -1 & 0 \\ 0 & -1 \end{bmatrix}$$

thus providing beam transport in the space between the RF cavities. At the same time this objective provides a condition for cancelling the deflection of unwanted particles in the second RF cavity. The condition $m_{21} = 0$ gives a cancellation of possible aberrations in the RF deflection structures;

f) the next objective, which focuses particles in such a way that it gives a minimal twisting of the phase-space ellipses in the vertical plane. This allows an increase of the efficiency of the collimators behind this objective. At the same time it helps to remove from the beam slow particles, muon background etc.;

g) the second momentum analyzer, which permits to clean the beam from unwanted particles and muon background;

h) the last objective, which transports particles to the bubble chamber focusing them in the horizontal plane in the centre of the chamber and making the beam parallel to the vertical plane. Experience shows that such a focusing is most useful for the subsequent analysis of bubble chamber pictures.

The characteristics of the above-mentioned elements are conditionned by the following circumstances :

a) As far as the target is concerned, the length of the target as mentioned above, should be approximately equal to one nuclear length, corresponding to the material used. The target cross-section depends on the desired momentum resolution, on the wanted acceptance and on possibility of producing the primary proton beam with the necessary characteristics. A target cross-section of 2 x 2 mm^2 is a suitable choice to meet all these requirements;

b) When calculating the first objective, one can use some CERN examples and adapt them to the higher momenta (e.g. U1).
However, such a scaling shows a loss of acceptance of about a factor of 4-5. Another solution was found for this objective, which reduced this loss to a factor of 1.6, and which gave a solid angle of $\sim 10^{-4}$ sterad. This objective consists of four 2m quadrupole lenses Q1-Q4, with an aperture of 20 cm, which are connected, relative to the focusing in the horizontal plane, in the following way :
FODODOF (F - focusing in the horizontal plane, D - defocusing in the horizontal plane, O - drift length).
More than 100 configurations were explored, and the solution proposed is the best found so far. For instance, some configurations would give a good acceptance, but not enough linear magnification for the subsequent momentum analysis. Conversely, other configurations would give a smaller acceptance but a good magnification. Table 6 shows a selected sample of the solutions found but not accepted.

c) The first momentum analyzer, consisting of 4 magnets M1-M4, and the field lens Q5 focusing horizontally, provide :
1) the maximum momentum resolution of $\pm$ 0.13 °/o;
2) that the most remote part of the channel is dispersion free.

d) The second objective, consisting of 2 quadrupoles Q7-Q8, is built according to the scheme FOD (which was chosen considering the aperture limitations) as is seen from Fig. 5.
The distance between these lenses was chosen according to the condition $m_{21} = 0$.

e) When calculating the optics between RF1 and RF2 (Q9-Q12), it is necessary to have in mind that this objective allows transport of particles between RF1 and RF2; the aperture of this objective must be big enough to permit the passage of particles with an inclination

TABLE 6

F - horizontal focusing

D - horizontal defocusing

M - bending magnet

O - drift length

A - length from the target up to centre of first lens (in meters)

B - length from the end of configuration up to horizontal image point

H - horizontal magnification

V - vertical magnification

Ω - acceptance (10^{-4} sterad)

Designed momentum p_o = 23 GeV/c

N	Configuration	A	B	Gradients / lens length (m) Q1	Q2	Q3	Q4	H	V	Ω
1	FODOFODOMOM	16	12	866/1	820/1	866/2	82092	2.25	0.86	0.2
2	FODODOFOMOM	10	12	911/1	875/2	875/1	911/2	0.97	4.03	0.6
3	FODOFODOMOM	10	12	874/2	752/2	874/2	752/2	4.62	1.13	0.6
4	FODODOFOMOM	16	12	826/1	777/2	777/1	826/2	0.75	2.63	0.3
5	FODOFODOMOM	10	12	600/1	600/1	1073/2	940/2	3.12	1.16	0.6
				etc.						

approximately twice as big as the one that results from the acceptance angle in the vertical plane (taking into account the additional deflection produced by the RF field in the RF1 cavity); the characteristics of this objective at the same time must allow us to make $m_{21} = 0$. All these requirements led us to the choice of the FODODOF scheme and to the computation of the gradients and drift lengths are given in Table 5.

f) The requirements of the objective Q13-Q16 were given above, and its calculation is not difficult. This objective is built according to the scheme DODOFOF. The choice of such a configuration resulted from the fact that the divergence of wanted particles is about 3 times more than was considered in the calculations of the acceptance angle. On the other hand, this objective must prepare the conditions for a good momentum resolution in the second momentum analyzer.

g) It was found, in the course of the calculation, that the necessary momentum resolutions which allow to clean properly the beam from muon contamination, can be obtained by means of an objective consisting of 4 lenses Q17-Q20 arranged according to the scheme DODOFOF, as well as by 2 magnets M5-M6, whose characteristics can be seen also in Table 5. For making this choice, the computations made for Q1-Q4 could again be used, as the requirements are similar.

h) The last objective, Q21-Q22, must provide a beam large enough for the bubble chamber. The choice of its characteristics depends on local conditions, and in particular on the parameters of the bubble chamber magnetic field, the distance available between the objective and the bubble chamber and so on. Therefore one can consider the characteristics of this objective as rather conventional.

To decrease the influence of non-linearity of quadrupole fields the whole calculation was made under the assumption that only 80% of the lens aperture was used.

Collimators and beam stopper are placed in the principal points of the channel, as shown on Fig. 5.

C1 collimator determining the acceptance in the horizontal plane placed at the focal point of the first quadruplet;

C2 collimator determining the acceptance in the vertical plane placed at the vertical focus in front of the first quadruplet;

C3 momentum slit, placed at the first horizontal image of the target;

C4 angle defining slit, placed at any convenient point before M3-M4;

C5 vertical collimator placed before the beam stopper and used for reducing the muon background; the setting of C5 and BS, relatively to the beam, is shown in Fig. 6.;

C6 vertical collimator, redefining the target dimensions, after the second RF cavity, and placed behind the Q13-Q16 objective;

C7 horizontal collimator, redefining the target dimension, x after the second RF cavity and placed behind the same objective;

C8 momentum slit of the second momentum analyzer (magnetic collimator);

C9 vertical collimator, defining the target dimensions in the vertical plane (magnetic collimator).

The role of these collimators is very important as far as the cleaning of the beam from muon background is concerned. As after them, in front of the bubble chamber, we have no additional momentum analyzers, the elimination of unwanted particles from the beam proves to be more effective if it is performed in a magnetized iron of up to 15-16 kgauss.

BS the beam stopper is placed just behind C5, in the front focusing point of the objective Q13-Q16.

The choice of the length of the beam stopper requires a more detailed knowledge of all characteristics of the optical elements of the channel. Thus the length of ~1 or 1.5 m seems to be rather reasonable.

The ray trajectories are shown in Fig. 5, where one can also see the collimators and the beam stopper positions.

A convenient scheme of channel power supply is shown in Fig. 7. Such optical and power supply schemes allow the use of the usual methods of beam tuning. Particular attention is drawn to current limits, giving a necessary stability of magnetic fields and gradients. Experience gained at CERN shows that, with the existing situation there, for a beam length of ~ 150-180 m, it is necessary to maintain currents in magnets and lenses with a stability not worse than 0.02 - 0.03%. Calculations of the SU-beam show that this value should be decreased to 0.010 - 0.015% (for magnets it has to be less or equal to 0.01%). For a compensation of a beam drift in the space between RF1 and RF2 due to this instability (~25-30 mm in the horizontal plane) one needs some special feed-back system for the M3-M4 magnets (small magnets or magnetic coils), which can be placed anywhere at the beginning of the space between RF1 and RF2.

The alignment of the optical elements should be performed with an accuracy not worse than 0.1 mm.

The construction of premises for such a beam of about 500 m is no simple economical and engineering problem. It requires a compilation of all local conditions and resources. An attractive proposal may be to use an open area for the channel - of an airport-runway-type - with a building at the end of the runway to accommodate the bubble chamber, and "prefab" barracks to accommodate equipment which is sensitive to climatic conditions.

Obviously, the beam layout presented here is not ideal, and needs further improvements. Such improvements, in the first place, must refer to increasing the first objective solid angle, and to seek for more effective optical combinations from the point of view of their simplicity and of a minimal level of the different aberrations. Of course, all phase spaces at the principal points of the channel (collimators, beam stopper, etc.) must be checked for a better determination of the characteristics of the beam elements, currents, tolerances and other conditions. However, this scheme can be considered as an initial step which can give a solution of the problem with an accuracy of ~5-10%.

Figure Captions

Fig. 1a. Principles of operation of the radiofrequency separator.

1b. Phase relations of two particles of different rest-masses with respect to the travelling wave.

Fig. 2. Cross-sections for π^+ and π^- production on Be at 0° by 50 and 70 GeV/c protons. A curve for 23.1 GeV/c protons is given for comparison.

Fig. 3 and Fig. 4 Expected particle intensities at the end of the beam.

Primary proton energy : 50 and 70 GeV/c.

The figures are calculated under the assumptions specified in the text.

Fig. 5. Optical layout and particle trajectories.

Fig. 6. Collimator C5 and beam stopper setting relative to the beam.

Fig. 7. Power supply circuit.

Fig. 8. Geometrical layout.

o o

o

References

1. M.M. Geiger, P. Lapostolle, B.W. Montague, CERN Rep. 61-26.

2. M. Bell, P. Bramham, R.D. Fortune, E. Keil, B.W. Montague, Int. Conf. on High Energy Accelerators, Dubna 1963, 798.

3. P. Bramham, R.D. Fortune, E. Keil, H. Lengeler, B.W. Montague, W.W. Neale, Phys. Lett., 15, 290 (1965)

4. W. Schnell, CERN Rep. 61-5.

5. Y. Garault, CERN Rep. 64-43.

6. B.W. Montague, CERN AR/Int. PSep/63-6.

7. U1 beam

9. G.H. Trilling, UCID-- 10148, 1965.

10. J. Ranft, Private communication.

    We thank Dr. Ranft for making these results available to us prior to publication.

11. D. Dekkers, J.A. Geibel, R. Mermod, G. Weber, T.R. Willits and K. Winter, Phys. Rev., 137, B962, (1965).

12. G. von Dardel, CERN NP/Int/62-17.

13. H. Lengeler, CERN/TC/BEAM 65-4.

14. P. Bramham, CERN Rep. 66-8, and E. Keil, CERN AR/Int PSep 63-3.

15. P. Bramham, CERN AR/Int PSep 65-9.

16. J.W. Gardner, D. Whiteside, NIRL/M/44, 1963.

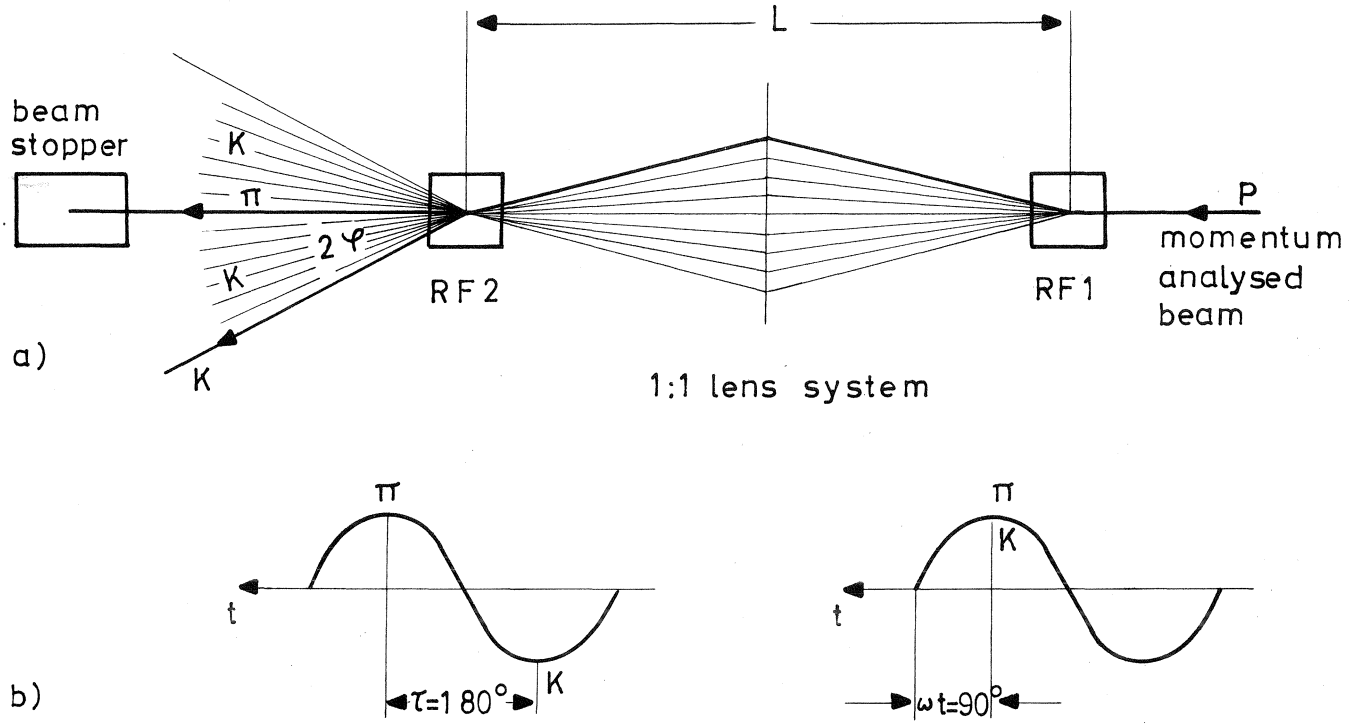
L
beam
stopper
K
π
2φ
K
K
RF 2
RF 1
P
momentum
analysed
beam
a)
1:1 lens system
b)
π
t
τ=180°
K
π
K
t
ωt=90°

fig. 1

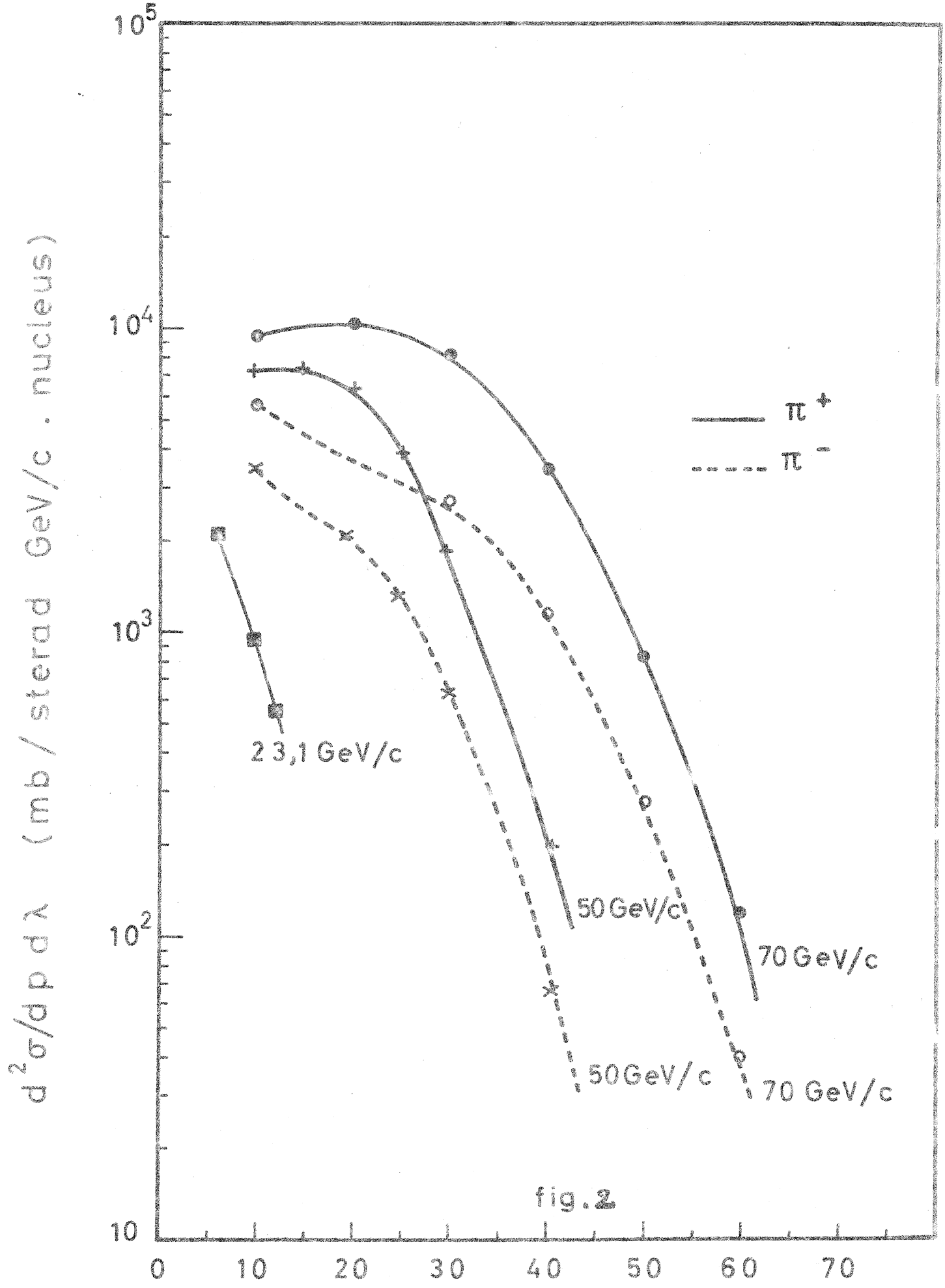
10^5
10^4
10^3
10^2
10
$d^2\sigma/dp\,p\,d\lambda$ (mb / sterad GeV/c . nucleus)
π^+
π^-
23,1 GeV/c
50 GeV/c
70 GeV/c
50 GeV/c
70 GeV/c
0
10
20
30
40
50
60
70
p GeV/c

fig. 2

PS/5292

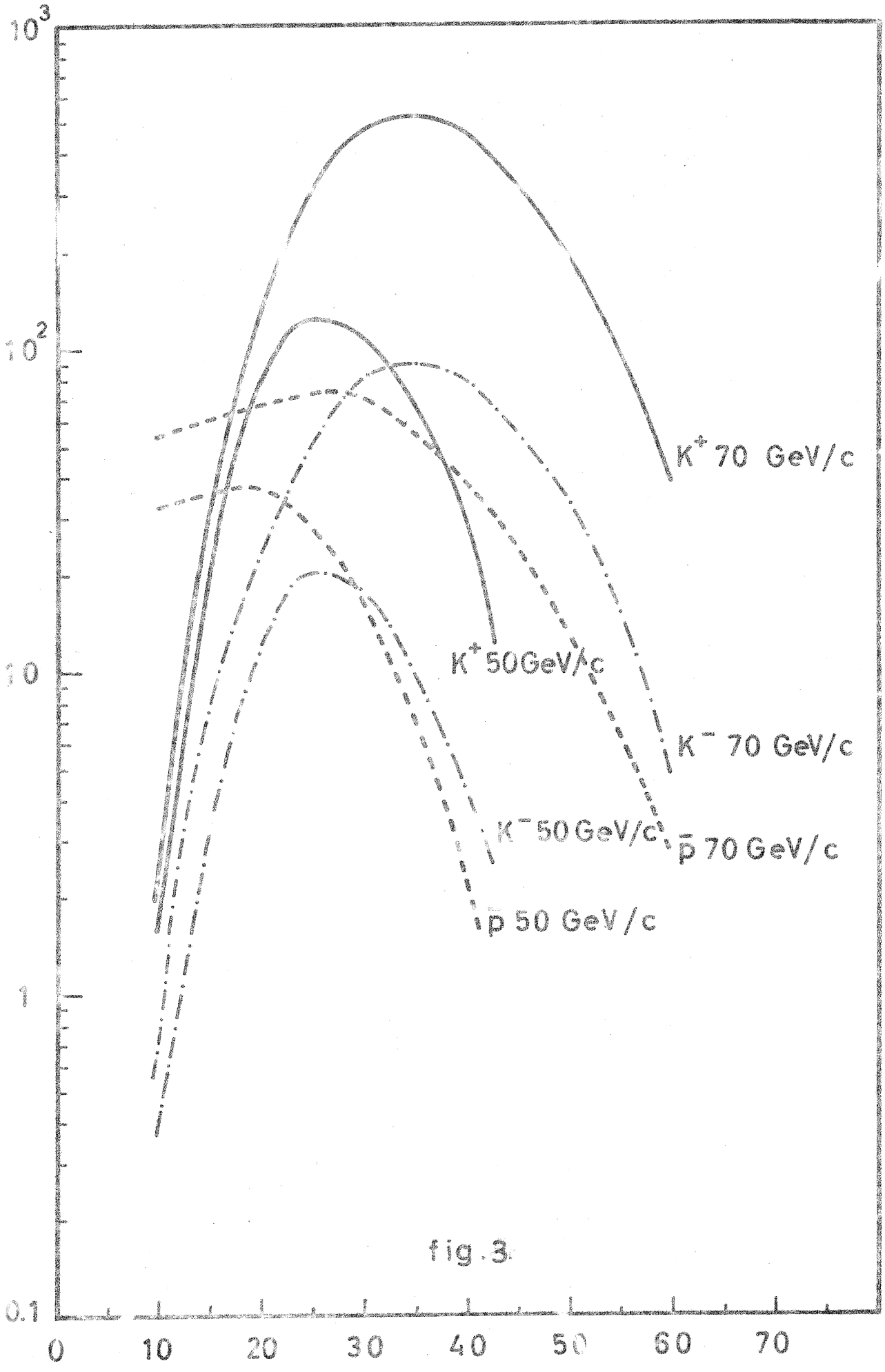
10^3
10^2
10
1
0.1
0
10
20
30
40
50
60
70
p GeV/c
K^+ 70 GeV/c
K^+ 50 GeV/c
K^- 70 GeV/c
K^- 50 GeV/c
$\bar{p}$ 70 GeV/c
$\bar{p}$ 50 GeV/c

fig. 3

PS/S292

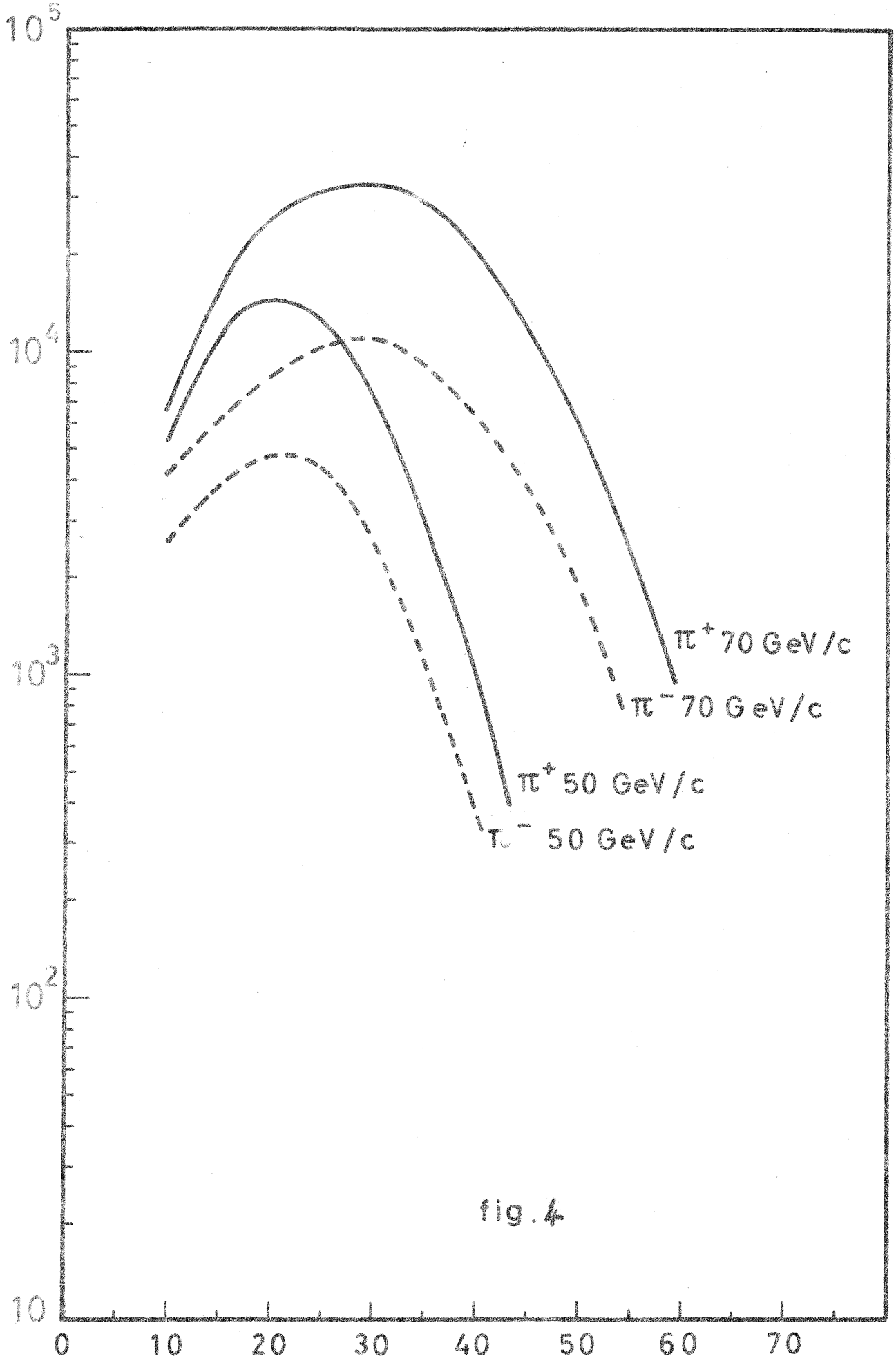
10^5
10^4
10^3
10^2
10
0
10
20
30
40
50
60
70
π^+ 70 GeV/c
π^- 70 GeV/c
π^+ 50 GeV/c
π^- 50 GeV/c
p GeV/c

fig. 4

PS/5292

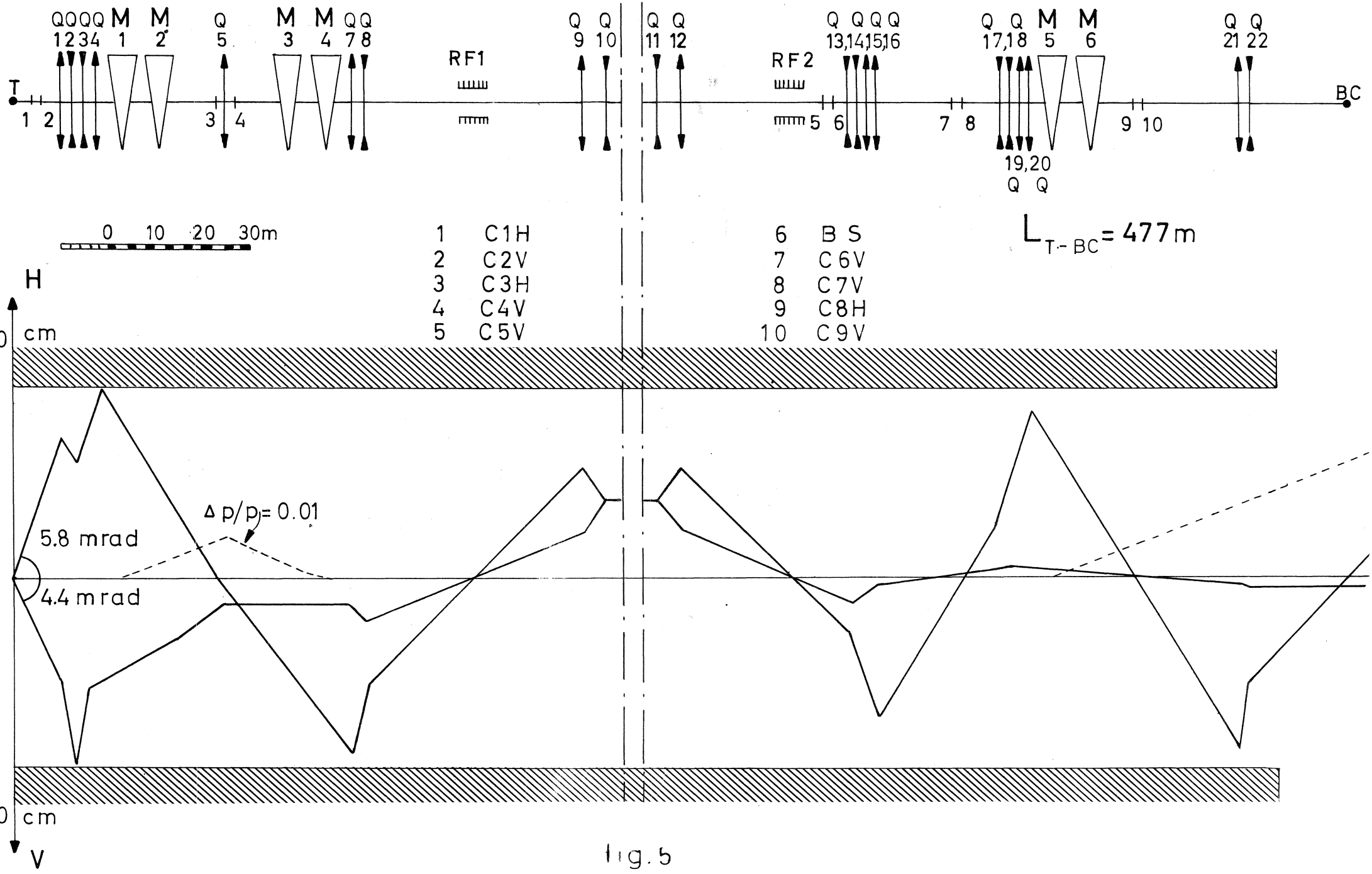

fig. 5

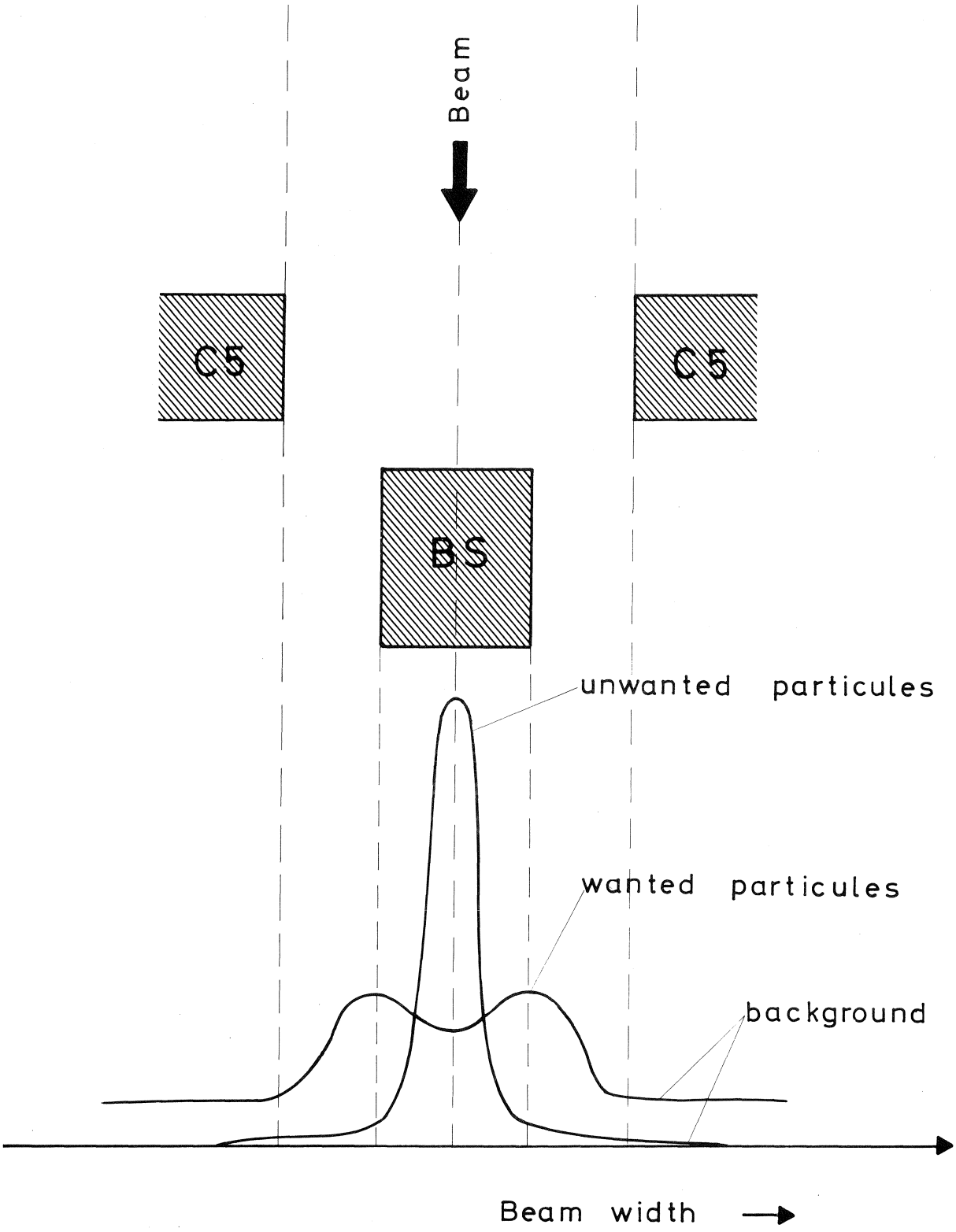
Beam
C5
C5
BS
unwanted particules
wanted particules
background
Beam width

fig . 6

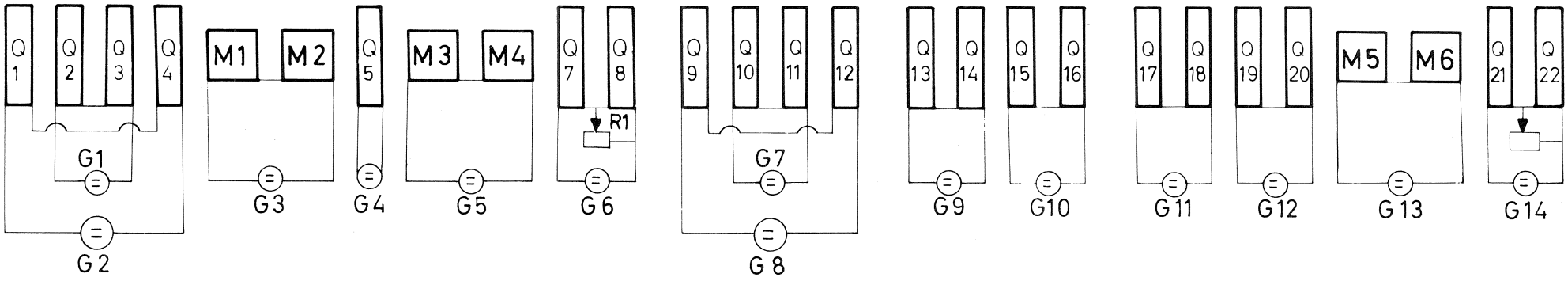

G - Generators

R - Rheostats

fig. 7

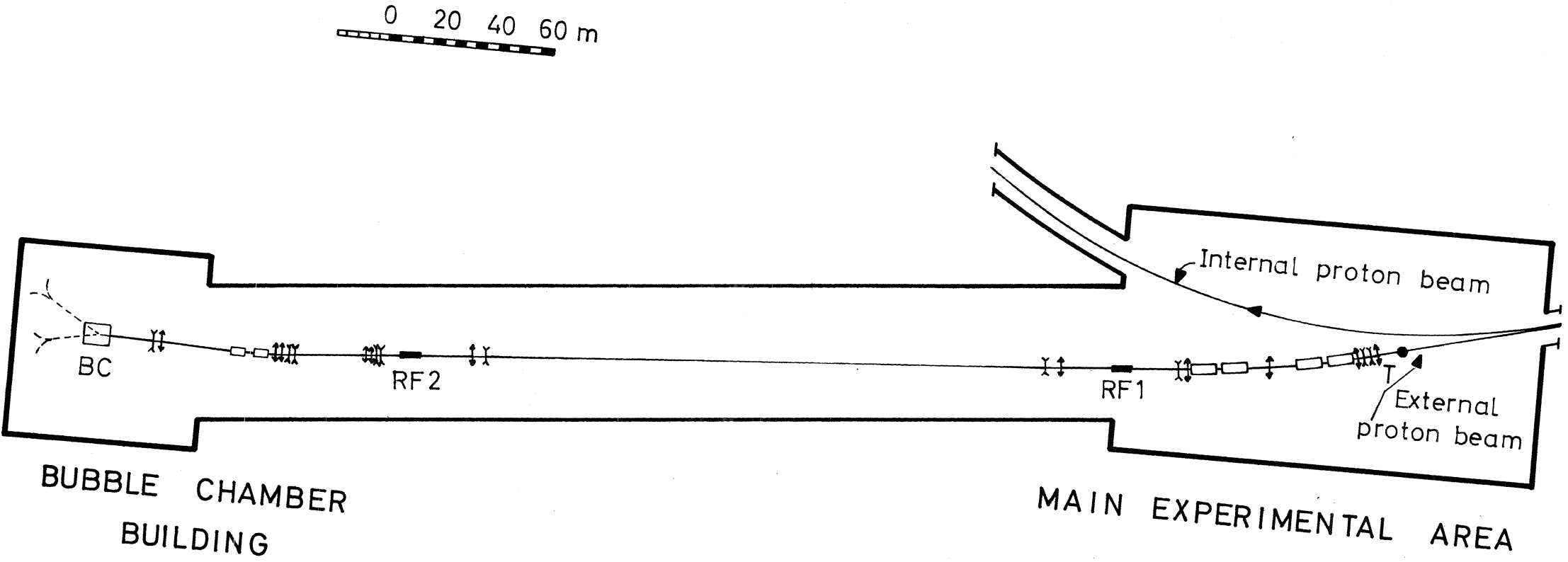
0 20 40 60 m
Internal proton beam
BC
RF2
RF1
T
External
proton beam
BUBBLE CHAMBER
BUILDING
MAIN EXPERIMENTAL AREA

fig. 8